

Freestanding diffractive optical elements as light extractors for burning plasma experiments

D. Stutman,^{1,a)} G. Caravelli,¹ M. Finkenthal,¹ G. Wright,² D. Whyte,³ N. Moldovan,⁴ R. Kaita,⁵ and L. Roquemore⁵

¹*Johns Hopkins University, Baltimore, Maryland 21218, USA*

²*University of Madison-Wisconsin, Madison, Wisconsin 53706-1418, USA*

³*Massachusetts Institute of Technology, Cambridge, Massachusetts 02139-4307, USA*

⁴*Northwestern University, Evanston, Illinois 60208, USA*

⁵*Princeton University, Princeton, New Jersey 08544, USA*

(Received 28 January 2008; accepted 6 March 2008; published online 15 May 2008)

Optical diagnostics will be critical for the operation and performance assessment of burning plasma experiments, such as ITER. At the same time, extracting light for these diagnostics with reflective mirrors becomes difficult in the burning plasma environment due to the deleterious effects of the prolonged exposure on plasma and nuclear radiations. As an alternative, we explore the possibility to use freestanding diffractive optical elements, such as transmission gratings and zone plates, as light extractors. Since in diffractive systems, light is deflected by periodic slits rather than by a surface, these may withstand plasma exposure with less degradation of their optical properties. To investigate this possibility, we developed freestanding transmission gratings for the visible range and exposed them to conditions resembling (or even exceeding) those expected for the ITER “first mirrors.” The results of this study indicate that the gratings can withstand high heat fluxes and plasma and energetic radiation bombardment. Additionally, in contrast to the reflective elements, the extraction efficiency of diffractive elements may even *improve* with plasma exposure, which is possibly due to the shaping and thinning of the grating bars by plasma erosion. Moreover, in tightly collimated configurations, even very thin gratings can be used to extract light from hot fusion plasmas, as demonstrated by our tests of an extreme ultraviolet extractor at the National Spherical Torus Experiment. © 2008 American Institute of Physics. [DOI: 10.1063/1.2919708]

I. INTRODUCTION

The magnetic fusion energy research is entering a new stage, in which the capability of producing a high fusion yield, near steady-state “burning” plasma will be demonstrated in advanced experiments, such as ITER.¹ Together with this step, a host of scientific and technological challenges arise. Among the most difficult is the accurate and reliable diagnostic of the plasma parameters needed for device operation, protection, and performance assessment. The challenge for the instrumentation lies in the harsh radiation environment (energetic neutron and gamma fluxes higher than in the core of a fission reactor), which is combined with the proximity to a very high temperature, long duration plasma (Ref. 2 and references therein).

Many essential diagnostics, such as those for the ion and electron temperature, impurity content, and current profile, are based on optical measurements. The spectral range involved is very broad, from the extreme ultraviolet (XUV) to the infrared (IR).² In the present designs, all these diagnostics rely on metallic mirrors (e.g., Mo and Au) for the extraction of useful light from the burning plasma.^{2,3} The mirror extractors combine the benefit of high efficiency with that of good resistance to nuclear radiation and heat loads. To avoid streaming of the fusion neutrons to outside the blanket, multiple mirrors are used in a labyrinth or “dog-leg” configura-

tion, in which a “first mirror” extracts the plasma light and then deflects it to a secondary, shielded mirror.²

This first mirror is also the most problematic; the reflective surface is exposed to a large flux of energetic neutral atoms escaping the plasma through charge exchange processes. Some of these atoms, such as deuterium, cause erosion through sputtering, while others such as C and Be can be deposited as thin films. The balance between erosion and deposition is strongly dependent on the mirror location, with erosion generally observed to dominate near the main, hot plasma, while deposition is dominant in the colder divertor. Both processes, however, adversely affect the mirror performance. Large changes in the mirror reflective and polarizing properties have been documented both in tokamak and *in situ* measurements.³⁻⁶

While ongoing studies focus on stabilizing the mirror properties and mitigating the surface erosion and deposition through shuttering and *in situ* cleaning, the challenges are substantial. In addition, there are many complex problems, such as possible synergistic effects between the nuclear and plasma radiations and the surface damage and/or deposition chemistry that still remain to be investigated.³

The first-mirror problem will be even more difficult in future fusion reactors: the intensity in nuclear radiation will increase by about an order of magnitude, device operation will be continuous, and access to the front end optics will not be possible for long periods of time. Given the importance of optical diagnostics for reactor operation, light extraction

^{a)}Electronic mail: stutman@pha.jhu.edu.

based on physical principles other than reflection needs to be explored as well. The concept we propose is using diffraction from freestanding optical elements, such as transmission gratings or Fresnel zone plates. Since diffractive optical elements deflect light by a periodic array of slits instead of a solid reflecting surface, there is a better chance that a diffractive extractor will maintain its optical properties during plasma and radiation exposure.⁷

There is also a larger choice of materials that can be used to make diffractive elements, since it is not the light reflection but rather the absorption properties that primarily govern their optical efficiency. For instance, an attractive material is tungsten, which has poor reflectivity but combines strong optical absorption with the highest resistance to sputtering among all materials.

Another advantage is that freestanding diffractive elements can operate near normal incidence, which makes them less sensitive to misalignment and may make easier remote replacement (e.g., through a simple parallel translation of a new diffractive surface). Freestanding diffractive optical elements are often used in synchrotron, plasma, and space XUV spectroscopic instrumentation.^{8–10}

The light extraction efficiency of freestanding diffractive elements can reach about 30%;⁸ however, for many burning plasma diagnostics (particularly for control related measurements), reliability and stability of the optical properties and photometric calibration may be more important than very high efficiency. Large area extractors can be made by using mosaics of diffractive elements, as it is done for space instrumentation.¹⁰ Furthermore, although the diffractive elements exhibit strong chromatic effects, most fusion optical diagnostics use a rather limited spectral range around a central wavelength (e.g., several tens of angstroms around the D_α line in the case of the motional Stark effect diagnostic). In addition, as illustrated in Sec. III, there are simple designs that enable extraction of a broad range of wavelengths. Last but not the least, an important advantage of the diffractive solution is that it is scalable with predictable and constant efficiency over a wide spectral range, in principle, from the XUV to the infrared.

Here, we present the first results of investigating the resilience to plasma and radiation exposure of large period ($d=4\ \mu\text{m}$), freestanding transmission gratings for the visible to near IR range. Such devices have large potential for the diagnostic of burning plasmas and were chosen first for the damage tests because of their less complex manufacturing process, as well as to simplify the experiments. Gratings made in Si were exposed to plasma and high energy ion bombardment, at levels similar or exceeding those predicted for the first mirrors in ITER. The tests were performed at the plasma-ion accelerator DIONISOS facility, which is developed for studies of fusion plasma facing components.¹¹

In addition to the DIONISOS experiments, an XUV light extractor, which uses a thin gold transmission grating, was installed close to the plasma of the National Spherical Torus Experiment (NSTX) at Princeton¹² and its performance was tested during a lithium wall conditioning campaign.

The paper is structured as follows. Section I briefly describes the pre-exposure characteristics of the visible trans-

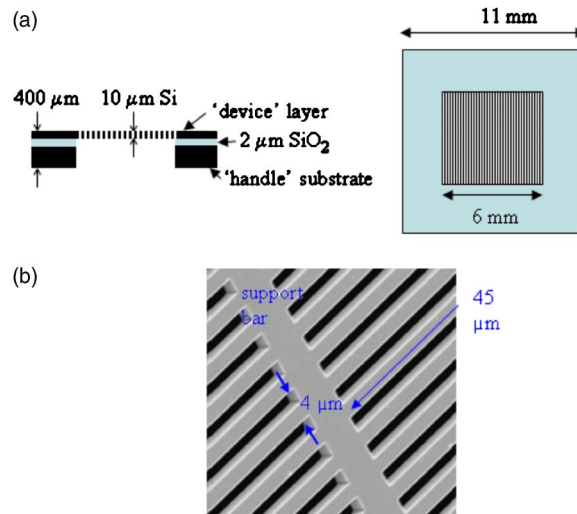


FIG. 1. (Color online) (a) Structure of freestanding transmission gratings made by the SOIMUMP process in silicon-on-oxide wafers. (b) Scanning electron microscopy image of finished grating.

mission gratings and presents the plasma exposure and ion irradiation experiments at DIONISOS, together with the results of the postexposure characterization. In Sec. II, we assess the effects of plasma coatings on the diffractive elements, discuss designs for imaging light extractors geared toward possible applications for burning plasma diagnostic, and present an example of XUV light extraction from the NSTX.

II. PLASMA EXPOSURE AND IRRADIATION TESTS

A batch of $4\ \mu\text{m}$ period, freestanding transmission gratings were manufactured in a 4 in. silicon wafer by MEMSCAP, USA by using silicon-on-oxide multiuser microelectromechanical processes or SOIMUMP.¹³ The structure of the gratings is shown in Fig. 1 and consists of a $400\ \mu\text{m}$ thick “handle” wafer, having on top a $2\ \mu\text{m}$ thick SiO_2 layer, followed by a $10\ \mu\text{m}$ thick “device” layer, and made of p -type silicon. The grating is made in the device layer, which have, thus, a thickness of $\approx 10\ \mu\text{m}$. The grating consists of alternating gaps (slits) and bars of $2\ \mu\text{m}$ width and $45\ \mu\text{m}$ height [Fig. 1(b)]. The bars are reinforced by a transversal grid of $5\ \mu\text{m}$ wide bars, which have $50\ \mu\text{m}$ period. The geometric open area of the grating is, thus, $\approx 45\%$. This spatial layout replicates the typical geometry of freestanding metallic transmission gratings for the soft x-ray range but is about twenty times larger.^{9,14} The Si gratings are also semiconducting, with an estimated resistivity of $\approx 10\ \Omega\ \text{cm}$. The total grating area is $6 \times 6\ \text{mm}^2$ and about 15 gratings were obtained from the 4 in. wafer.

The diffraction efficiency of the gratings was accurately calibrated in the laboratory to characterize them prior to the irradiation tests. The experimental calibration is necessary because, due to the complexity of light interaction with a semiopaque, semiconducting three-dimensional microstructure, it is difficult to accurately predict the grating transmission, particularly for polarized light, at wavelengths comparable to the grating period and at incidence angles away from the normal.^{14–17} For instance, at a few degrees off normal

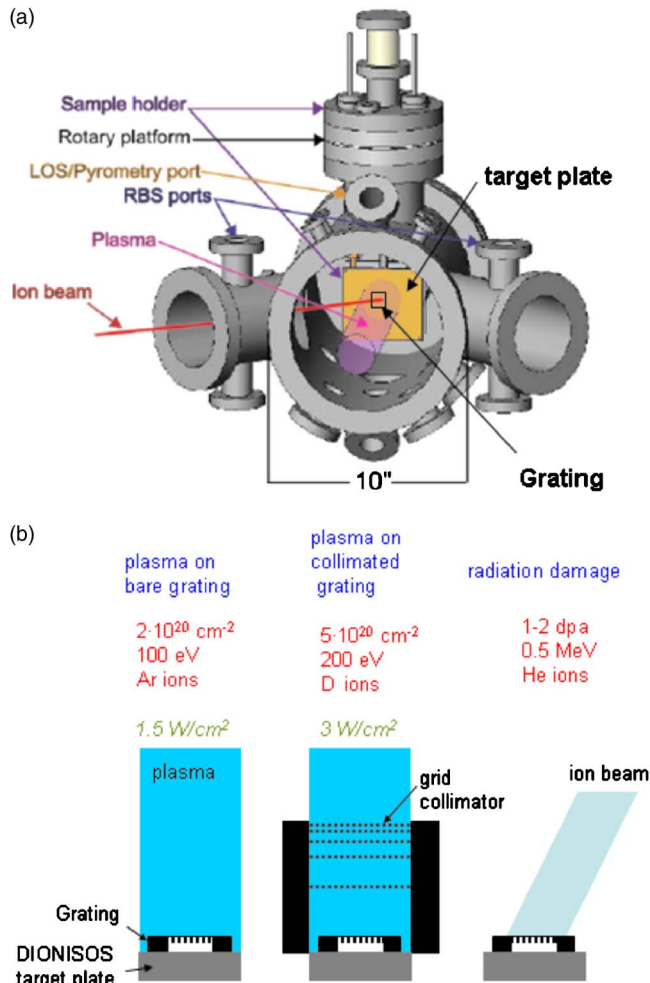


FIG. 2. (Color online) (a) Layout of the DIONISOS facility (Ref. 11). (b) Exposure conditions for the freestanding Si gratings.

incidence, our gratings exhibit a strong waveguiding or “blaze” effect that nearly doubles the grating efficiency in the first order and increases it by about an order of magnitude in the second order. Similar effects have been observed with gratings for the XUV range.^{18,19}

The DIONISOS facility is designed to combine intense plasma exposure of a plasma facing component, with *in situ* ion beam analysis of the exposed surface.¹¹ It consists of a steady-state helicon source that produces a 2–5 eV temperature, high-density ($\leq 10^{13}$ cm⁻³) plasma column of ≈ 50 mm diameter, which is extracted through a 1 kG solenoid field to a target chamber. Biasing of the target allows for control of the incident ion energy in the range of 10–500 eV. The target chamber is attached to a dual-source 1.7 MV tandem ion accelerator that can supply MeV light and heavy ion beams [Fig. 2(a)]. The areal coverage of the ion beam on the grating is controlled by electrostatic raster scanning or by changing the beam focusing.

The exposure conditions in our experiments were chosen to resemble those for first mirrors operating near the main ITER plasma. As mentioned above, the first optical elements in the burning plasma are exposed to several environmental factors: heat loads arising from plasma and nuclear radiation, erosion by sub-keV charge exchange atoms (CXAs), bom-

bardment by multi-MeV neutrons and gamma rays, and deposition of thin films of low- and high-Z atoms. The peak heat load predicted for ITER first mirrors is around 0.15 W/cm².²⁰ The CXA fluxes are predicted to reach $\approx (1-2) \times 10^{15}$ deuterium atoms/cm² for the mirrors closest to the outer wall, with an average energy of $\approx 250-350$ eV.^{2,4} Assuming a discharge duration of several hundred seconds, the ion fluence expected after 10³ ITER discharges (about one calendar year of operation) will, thus, be 4×10^{20} atoms/cm². At this fluence, erosion of the first micron or so from optical surfaces can occur.^{3,4} In addition, radiation damage of the bulk and subsurface material of up to ≈ 1 dpa (dpa denotes displacements per atom) can be expected, which is due primarily to bombardment with energetic neutrons.²

In the simulation of the first-mirror-like conditions, we used three experimental arrangements [Fig. 2(b)]: the first consisted of directly exposing a bare grating to bombardment with argon plasma, with a target bias of -100 V to have Ar ions with ≈ 100 eV energy impacting the surface. The aim of this experiment was to erode the first few microns from the grating optical surface. We exposed the grating to a fluence of $\approx 2 \times 10^{20}$ cm⁻² of 100 eV Ar⁺ ions, which was computed with the SRIM code²¹ to sputter ≈ 2 μ m from the Si surface. In addition, to arrive at this fluence, we used a large ion flux of $\approx 10^{17}$ cm⁻² s⁻¹ that produced an order of magnitude higher heat load on the grating (≈ 1.5 W/cm²) than that expected for the ITER first mirrors.

The second arrangement consisted of exposing a grating to conditions that simulate its operation as a light extractor in a spectroscopic diagnostic, i.e., behind a collimator that limits the viewing angle in the dispersion direction (see Sec. III and Ref. 7). The collimator consisted of thin Mo foils having arrays of slits that limited the plasma viewing angle to $\approx 10^{-3}$ sr.²² In this arrangement, the grating was subjected to a fluence of 5×10^{20} cm⁻² of 200 eV D⁺ ions, which is equivalent to the CXA impact from more than a thousand ITER discharges. In addition, the average ion flux on the device was 10^{17} cm⁻² s⁻¹, which produces a heat load of ≈ 3 W/cm².

Finally, a bare grating was exposed to a 0.5 MeV He⁺ ion beam, which is oriented at $\approx 45^\circ$ with respect to the grating surface. To cover the grating area, we used a diffuse (5–6 mm diameter) beam spot. This setup was meant to simulate energetic neutron damage in the first micron layer below the grating surface. The simulation of neutron damage to optical surfaces by using bombardment with MeV ions is discussed in Ref. 23. The grating was subjected to a fluence of $\approx 3.6 \times 10^{16}$ ions/cm² that, according to the SRIM calculation, produced $\approx 1-2$ dpa material damage in the first micron under the grating surface.

Following the DIONISOS tests, the efficiency of the gratings was measured by using the same procedures used for the pre-exposure characterization. The first important result is that the exposure to heat loads well in excess of those expected in ITER did not “burn” or otherwise damage the thin Si gratings. This should not be surprising after all, since

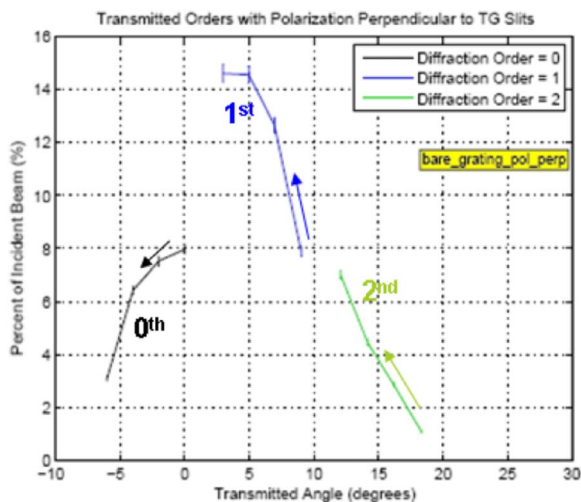


FIG. 3. (Color online) Efficiency for 6328 Å polarized light of the bare grating exposed to 100 eV Ar plasma. The arrows indicate the direction of efficiency change as the incidence angle departs from normal.

the device layer in which the gratings were made is designed to withstand heat loads of several W/cm^2 in high power electronic devices.

The second important result is that the plasma erosion and energetic ion irradiation did not adversely affect the optical properties of the gratings. Thus, the postexposure calibration at 4360 Å of a bare grating eroded by 100 eV Ar ions showed an efficiency of $6\% \pm 0.3\%$ in the first order at normal incidence and $11\% \pm 0.3\%$ at the incidence angle corresponding to the maximum of the waveguiding effect. Compared to the pre-exposure values of $5.3\% \pm 0.3\%$ and $10\% \pm 0.3\%$, respectively, this indicates that the blue light grating efficiency slightly *increased* following the plasma exposure. Such an increase may be explained by the shaping of the grating bars by the plasma erosion. Indeed, as discussed in Ref. 24, gratings with rounded bar edges have somewhat higher efficiency than gratings with perfectly rectangular bars. The postexposure efficiency of the Ar^+ sputtered grating measured in red light also stayed high, as shown in Fig. 3. A several percent change in efficiency compared to that measured in the pre-exposure experiments was observed, which may be attributed to phase effects arising from the thinning of the grating by plasma erosion; these effects become significant at red wavelengths where Si is partly transmissive.^{14,15}

Similar results were obtained for the gratings exposed to 200 eV D^+ plasma bombardment and to 0.5 MeV He^+ ion irradiation. Their postexposure efficiency for blue light was $10.2\% \pm 0.3\%$ (at the blaze angle), i.e., unchanged from the pre-exposure values within the measurement error. The reduced particle fluence in these configurations is not expected to significantly modify the shape or thickness of the bars.

III. DIFFRACTIVE OPTICAL ELEMENTS AS LIGHT EXTRACTORS FOR BURNING PLASMAS

A. Effects of plasma coatings

The above results are encouraging for the application of diffractive optical elements as light extractors in the burning

plasma environment. Given that silicon gratings could withstand levels of plasma exposure and radiation damage comparable to those in ITER, one can infer that diffractive elements made of heavy refractory metals or ceramics would resist for long periods of time in close proximity to the burning plasma. Assuming, for instance, a tungsten grating extractor operated near the ITER first wall (CXA flux of 2×10^{15} atoms $\text{cm}^{-2} \text{s}^{-1}$ of 350 eV mean energy at midplane^{2,4}), together with a modest reduction (e.g., by a factor of 3) in the CXA flux due to baffling or collimation, the grating would be thinned over the ITER lifetime by $\approx 0.1\text{--}0.2$ μm . As suggested by the above results, this level of erosion should not affect the diffraction efficiency even for gratings much thinner than those we tested, likely down to a fraction of micrometer bar thickness. Assuming the same ratio of about 20:1 between the grating thickness and the characteristic wavelength of operation, diffractive extractors with baffling or collimation could be used in the burning plasma starting from the XUV spectral range.⁷ This conclusion is also supported by the NSTX results that will be discussed below.

A question which we could not directly address in the DIONISOS experiments relates to the effect of thick plasma coatings on the optical properties of the diffractive extractors. Since any laboratory plasma exposure results in surface contaminants, the DIONISOS results indicate that thin coatings have no negative impact on the gratings. However, as mentioned above, thick (micron range) coatings of low- and high-Z impurities are anticipated for the ITER first mirrors. While such films have a strong impact on the reflective and polarization properties of metallic mirrors,²⁻⁶ one can expect a much reduced effect on the freestanding diffractive elements. The magnitude of this effect can be estimated by including in the diffraction efficiency calculation the light absorption and phase shift due to the additional deposited layer. As an illustration, we computed by using the grating model in Refs. 14 and 15 the efficiency of thin (1 μm) and thick (10 μm) Si gratings of 4 μm period, which operate at wavelengths around 4300 Å and coated with amorphous hydrogenated C films of thickness up to 1 μm . By using the measured optical constants of plasma deposited carbon films,²⁵ one obtains a relative efficiency variation of at most 10% for the 1 μm thick grating, while the efficiency change is entirely negligible for the 10 μm thick grating (Fig. 4). The same approach shows that for a grating made of a strongly absorbing material such as tungsten, the efficiency change will be negligible over a broad range of gratings and film thicknesses.

B. Designs for imaging diffractive light extractors

One can, therefore, envision plasma and radiation resistant diffractive light extractors from the XUV to the IR range. Their efficiency could be maximized for a given spectral domain by optimizing the waveguiding and phase effects; how the optical layout of such extractors would look will depend on the specific application and whether nonfocusing (transmission gratings) or focusing (zone plates) diffractive elements are used. For instance, a simple layout for a

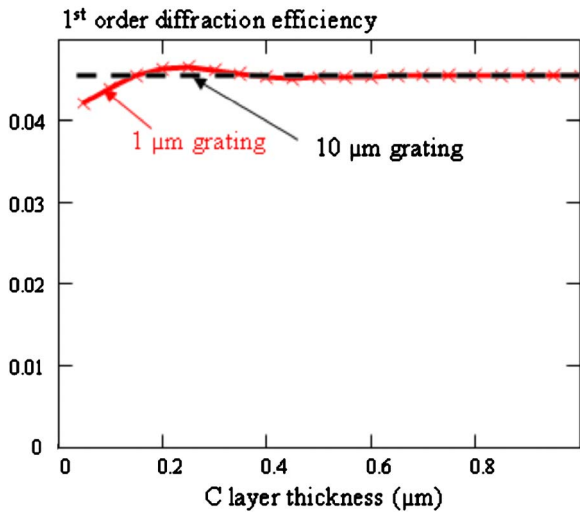


FIG. 4. (Color online) Computed effect of an increasing thickness of amorphous hydrogenated carbon deposition on a $1\ \mu\text{m}$ thin Si grating and on a $10\ \mu\text{m}$ thick grating. A wavelength of $4300\ \text{\AA}$ in the first order and a $4\ \mu\text{m}$ grating period were assumed in the computation.

transmission grating based extractor is to collimate the plasma light in the dispersion direction and use the perpendicular direction for spatial imaging.⁷ The use of this configuration for spectrally resolved imaging of impurity XUV emission from a small tokamak is described in Ref. 9.

Many important fusion diagnostics are based on visible to IR emission, which can be more easily relayed out of the vessel for remote analysis with high resolution spectrometers. It is, thus, of interest to explore diffractive extractor configurations, in which the diffracted light is relayed by using conventional, reflective or refractive secondary optics. In a fusion reactor, this configuration would ensure that only the freestanding diffractive element is exposed to the plasma, while the secondary relay optics are protected everywhere from erosion or deposition.

To illustrate this possibility, we tested a simple optical setup, which consists of an extended spectral source, a set of collimating slits, a freestanding Si grating at normal incidence, and a focusing lens playing the role of relay or secondary optical element [Fig. 5(a)]. The extracted light was intercepted on a screen and photographed with a charge coupled device camera. As seen in Fig. 5(a), in this arrangement, the secondary optical element does not directly view the light source.

The image of the source on the collecting screen is shown in Fig. 5(b) and illustrates that efficient light extraction, simultaneous with one-dimensional spatial imaging is feasible in this geometry, over a quite broad spectral range. In addition, the extracted light can be deflected by an even larger angle from the direct view of the source, using the strong waveguiding effect of the second order, mentioned in Sec. II.

Imaging light extractors, such as the one described above, should be of high interest for use in the ITER divertor. There, multichordal high resolution spectroscopy is required for the measurement of the impurity and working ion density, influx, and temperature. It is in the divertor, however, where mirror based extractors are most seriously

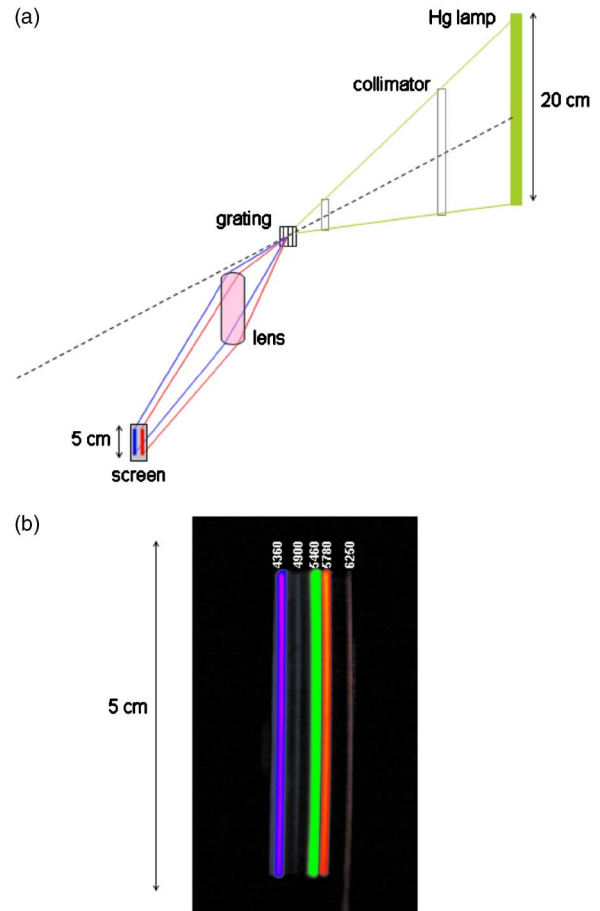


FIG. 5. (Color online) (a) Layout of transmission grating based imaging light extractor. (b) Space resolved image of the source on the collecting screen; the approximate wavelengths in angstrom are shown for the strongest Hg I lines.

challenged due to the intensity of the deposition effects.²⁻⁶ Extractors composed of a diffractive first element and secondary mirrors that relay the diffracted light to the outside instrumentation would be far less sensitive to plasma coatings.

In addition to extractors based on nonfocusing grating/focusing mirror combinations, one can envision also extractors directly based on focusing diffractive optics. These would combine the resistance to plasma exposure with an increased optical throughput. Focusing in one dimension can be achieved by varying the grating period and gap width along the dispersion direction,²⁶ while two-dimensional focusing can be obtained by using curvilinear zone plates.²⁷ An attractive spectral region to use with freestanding zone plates is the IR. Here, large “metallic lenses” could be envisioned that would withstand even the harshest plasma conditions. For instance, by scaling to IR wavelengths, the geometry of zone plates optimized for XUV [e.g., outermost zone width $\delta r_N \approx 400\ \text{\AA}$, 500 zones, zone plate thickness of $\approx 2000\ \text{\AA}$, and diameter $\approx 80\ \mu\text{m}$ (Ref. 8)], one obtains an IR zone plate lens having diameter of several centimeters, outermost zone width of a few tens of micrometers, thickness of a fraction of a millimeter, and focal length of around 1 m. Such zone plate lenses could be made in sputter resistant tungsten and would, thus, withstand almost direct plasma exposure,

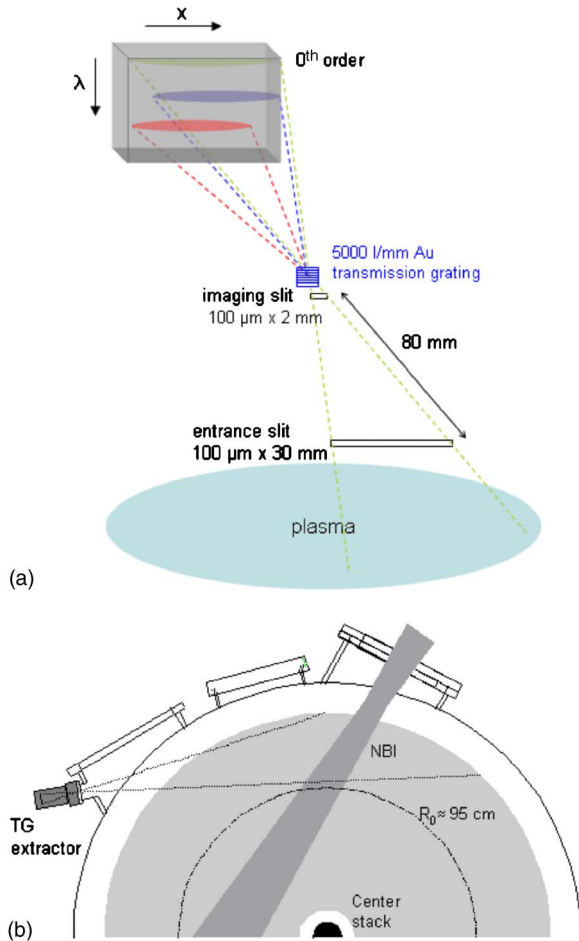


FIG. 6. (Color online) (a) Optical layout and (b) viewing geometry of XUV light extractor installed at NSTX. The figure depicts NSTX in the midplane horizontal cross section. R_0 is the major radius of the plasma magnetic axis, the center stack is the tube enclosing the toroidal field and induction coils, while the dark diagonal column marked with NBI indicates the path of the 100 keV neutral deuterium beams used to heat the plasma.

while collecting and focusing large amounts of IR light. An example of a critical application where such lenses could replace the first mirrors is IR thermography of the divertor.²⁸ The diagnostic needs to monitor with high space and time resolution (3 mm and 20 μ s, respectively) the temperature of the divertor plates. This requires close proximity to the divertor, together with good light collection efficiency. As for divertor spectroscopy, while using mirrors for light extraction is problematic due to deposition processes, using free-standing zone plates as first optical elements would largely alleviate this problem.

C. Application to XUV light extraction in NSTX

To test the functioning of extractors based on very thin gratings near a hot fusion plasma, we recently implemented at NSTX an extractor for the 10–50 Å range and used it to monitor the emission of both low- and high-Z impurities [Fig. 6(a)]. The extractor is based on a 2000 Å period, 0.3 μ m thick gold transmission grating that deflects the fan shaped beam defined by two collimating slits, each having 100 μ m width and separated by 8 cm. The extracted beam is intercepted by a XUV-to-visible light converter consisting of

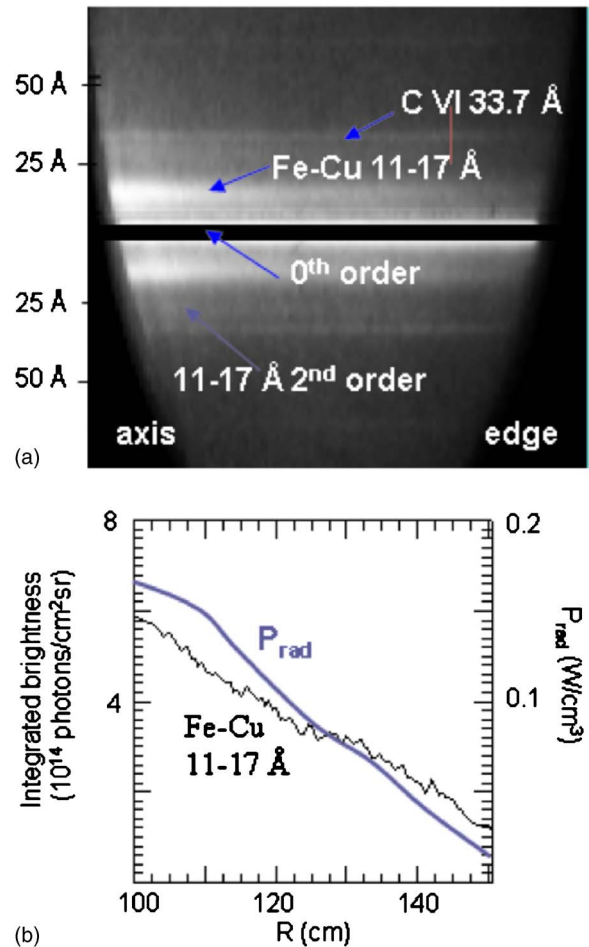


FIG. 7. (Color online) (a) Spectrally and space resolved XUV emission from a NSTX high confinement (H-mode) plasma, which is obtained by using the transmission grating extractor in Fig. 6. (b) Comparison between the 11–17 Å brightness profile measured by the XUV extractor and the radiated power profile measured by bolometer; the radial coordinate in the extractor plot represents the tangency radius of the viewing chord.

a thin layer of columnar CsI:Tl.²⁹ The visible light was recorded with an image intensifier/complementary metal oxide semiconductor array combination. A similar design was used by Wilhein *et al.* to image the soft x-ray emission from laser produced plasmas.³⁰ The extractor viewed the neutral heating beams [Fig. 6(b)] to also include in the measurement the charge exchange excited XUV line emission. In the case of low-Z impurities, such as C, this is the dominant emission from the core. The spatial resolution of the device is of a few centimeters.

To maximize the light collection efficiency and spatial resolution, the device was installed with its input slit close to the plasma [Fig. 6(b)]. Despite the close proximity to the hot and dense plasma, the thin XUV grating maintained its functionality throughout the NSTX operation, which includes a Li wall conditioning campaign, in which large amounts of Li were evaporated into the plasma and the wall was coated with Li films. The functioning of the extractor is illustrated in Fig. 7(a) for a discharge contaminated by metals. The spectrally resolved image shows good discrimination between the *L*-shell emission of metallic impurities in the \approx 11–17 Å range (Fe to Cu) and the C VI Ly_α emission at

33.7 Å. The relatively strong background is not due to the grating but to the high sensitivity of the CsI:Tl converter to the scattered gamma photons.

In addition to spectral discrimination, the space resolving capability of the extractor enables us to put in evidence a strong peaking of the metallic *L*-shell emission in the center of the plasma [Fig. 7(b)]; the *C* emission is more uniformly distributed. The central peaking of the metal emission is also indicated by the radiated power profile. The calculations of the metallic impurity distribution show, indeed, that at the electron temperature in these plasmas ($T_{e0} \leq 1$ keV) and with typical impurity transport coefficients in NSTX H modes,³¹ the *L*-shell charge states of elements from Fe to Cu are expected to peak in the plasma center. On the other hand, the *C* density profile measured by visible charge exchange spectroscopy evolves from hollow to flat during this discharge, which is consistent with the rather uniform C VI Ly α distribution recorded by our extractor.

IV. CONCLUSIONS

Our initial assessment of the resistance to damage of freestanding diffractive optical elements shows almost unchanged (or even slightly improved) efficiency after intense plasma and energetic ion bombardment. Such an improvement can, indeed, occur due to shaping and thinning of the grating bars by the plasma and could eventually be “built-in” in the design of the diffractive element.

Concerning the effect of plasma coatings, although more tokamak experiments are needed for a definitive statement, our calculations and the NSTX results suggest that they should have much less of an impact than for reflective optics. Thus, while the light collection efficiency is lower for diffractive extractors than for reflective ones, the stability of their optical properties and photometric calibration may be more important, in particular, for plasma control and machine protection measurements. In addition, the flexibility in optical design and material choices offered by the diffractive optical elements makes them an interesting alternative to the reflective optics for burning plasma diagnostic and control.

ACKNOWLEDGMENTS

This work is supported by U.S. DOE Grant No. DE-FG02-99ER54523.

¹M. Shimada, D. J. Campbell, V. Mukhovatov, M. Fujiwara, N. Kirneva, K. Lackner, M. Nagami, V. D. Pustovitov, N. Uckan, J. Wesley, N. Asakura, A. E. Costley, A. J. H. Donné, E. J. Doyle, A. Fasoli, C. Gormezano, Y. Gribov, O. Gruber, T. C. Hender, W. Houlberg, S. Ide, Y. Kamada, A. Leonard, B. Lipschultz, A. Loarte, K. Miyamoto, V. Mukhovatov, T. H. Osborne, A. Polevoi, and A. C. C. Sipps, *Nucl. Fusion* **47**, S1 (2007).

²A. J. H. Donné, A. E. Costley, R. Barnsley, H. Bindslev, R. Boivin, G. Conway, R. Fisher, R. Giannella, H. Hartfuss, M. G. von Hellermann, E. Hodgson, L. C. Ingesson, K. Itami, D. Johnson, Y. Kawano, T. Kondoh, A. Krasilnikov, Y. Kusama, A. Litnovsky, P. Lotte, P. Nielsen, T. Nishitani, F. Orsitto, B. J. Peterson, G. Razdobarin, J. Sanchez, M. Sasao, T. Sugie, G. Vayakis, V. Voitsenya, K. Vukolov, C. Walker, K. Young, and the ITPA Topical Group on Diagnostics, *Nucl. Fusion* **47**, S337 (2007).

³A. M. Litnovsky, V. S. Voitsenya, A. E. Costley, and A. J. H. Donné, *Nucl. Fusion* **47**, 833 (2007).

⁴A. Litnovsky, P. Wienhold, V. Philipps, G. Sergienko, O. Schmitz, A. Kirschner, A. Kreter, S. Droste, U. Samm, Ph. Mertens, A. H. Donné, TEXTOR Team, D. Rudakov, S. Allen, R. Boivin, A. McLean, P. Stangeby, W. West, C. Wong, DIII-D Team, M. Lipa, B. Schunke, Tore-Supra Team, G. De Temmerman, R. Pitts, TCV Team, A. Costley, V. Voitsenya, K. Vukolov, P. Oelhafen, M. Rubel, and A. Romanyuk, *J. Nucl. Mater.* **363–365**, 1395 (2007).

⁵V. S. Voitsenya, *AIP Conf. Proc.* **812**, 211 (2006).

⁶A. Litnovsky and V. S. Voitsenya, in Proceedings of the 12th ITPA Meeting on Diagnostics, Princeton, 2007 (unpublished).

⁷D. Stutman, M. Finkenthal, G. Suliman, K. Tritz, L. Delgado-Aparicio, R. Kaita, D. Johnson, V. Soukhanovskii, and M. J. May, *Rev. Sci. Instrum.* **76**, 023505 (2005).

⁸See <http://xrada.com> for typical optical properties of freestanding Zone Plates.

⁹B. Blagojevic, D. Stutman, M. Finkenthal, H. W. Moos, R. Kaita, and R. Majeski, *Rev. Sci. Instrum.* **74**, 1988 (2003).

¹⁰C. Canizares, J. E. Davis, D. Dewey, K. A. Flanagan, E. B. Galton, D. P. Huenemoerder, K. Ishibashi, T. H. Markert, H. L. Marshall, M. McGuirk, M. L. Schattenburg, N. S. Schulz, H. I. Smith, and M. Wise, *Publ. Astron. Soc. Pac.* **117**, 1144 (2005).

¹¹G. M. Wright, D. G. Whyte, B. Lipschultz, R. P. Doerner, and J. G. Kulpin, *J. Nucl. Mater.* **363–365**, 977 (2007).

¹²M. Ono, S. M. Kaye, Y.-K. M. Peng, G. Barnes, W. Blanchard, M. D. Carter, J. Chrzanowski, L. Dudek, R. Ewig, D. Gates, R. E. Hatcher, T. Jarboe, S. C. Jardin, D. Johnson, R. Kaita, M. Kalish, C. E. Kessel, H. W. Kugel, R. Maingi, R. Majeski, J. Manickam, B. McCormack, J. Menard, D. Mueller, B. A. Nelson, B. E. Nelson, C. Neumeyer, G. Oliaro, F. Paolotti, R. Parsells, E. Perry, N. Pomphrey, S. Ramakrishnan, R. Raman, G. Rewoldt, J. Robinson, A. L. Roquemore, P. Ryan, S. Sabbagh, D. Swain, E. J. Synakowski, M. Viola, M. Williams, J. R. Wilson, and NSTX Team, *Nucl. Fusion* **40**, 557 (2000).

¹³See <http://www.memscap.com>.

¹⁴H. W. Schnopper, L. P. Van Speybroeck, J. P. Delvaille, A. Epstein, E. Killne, R. Z. Bachrach, J. Dijkstra, and L. Lantward, *Appl. Opt.* **16**, 1088 (1977).

¹⁵K. Eidmann, M. Kühne, P. Müller, and G. D. Tsakiris, *J. X-Ray Sci. Technol.* **2**, 259 (1990).

¹⁶E. E. Scime, E. H. Anderson, D. J. McComas, and M. L. Schattenburg, *Appl. Opt.* **34**, 648 (1995).

¹⁷M. M. Balkey, E. E. Scime, M. L. Schattenburg, and J. van Beek, *Appl. Opt.* **37**, 5087 (1998).

¹⁸N. M. Ceglio, *J. X-Ray Sci. Technol.* **1**, 7 (1989).

¹⁹D. R. McMullin, D. L. Judge, C. Tarrío, R. E. Vest, and F. Hanser, *Appl. Opt.* **43**, 3797 (2004).

²⁰A. E. Costley, D. J. Campbell, S. Kasai, K. E. Young, and V. Zaveriaev, *Fusion Eng. Des.* **55**, 331 (2001).

²¹See <http://www.srim.org>.

²²V. A. Soukhanovskii, D. Stutman, M. Finkenthal, H. W. Moos, R. Kaita, and R. Majeski, *Rev. Sci. Instrum.* **72**, 3270 (2001).

²³V. Voitsenya, V. G. Kononov, A. F. Shtan', S. I. Solodovchenko, M. F. Becker, A. F. Bardamid, K. I. Yakimov, V. T. Gritsyna, and D. V. Orlinski, *Rev. Sci. Instrum.* **70**, 790 (1999).

²⁴F. Paerels, S. Kahn, and D. Wolkovitch, *Astrophys. J.* **496**, 473 (1998).

²⁵S. Lin and S. Chen, *J. Mater. Res.* **2**, 645 (1987).

²⁶C. David, B. Nohammer, and E. Ziegler, *Appl. Phys. Lett.* **79**, 1088 (2001).

²⁷G. Schmahl, D. Rudolph, P. Guttman, and O. Christ, in *X-Ray Microscopy*, edited by G. Schmahl and D. Rudolph (Springer-Verlag, Berlin, 1984), Vol. 43, pp. 63–74.

²⁸K. Itami, T. Sugie, G. Vayakis, and C. Walker, *Rev. Sci. Instrum.* **75**, 4124 (2004).

²⁹L. Delgado-Aparicio, D. Stutman, K. Tritz, R. Vero, M. Finkenthal, G. Suliman, R. Kaita, R. Majeski, B. Stratton, L. Roquemore, and C. Tarrío, *Appl. Opt.* **46**, 6069 (2007).

³⁰T. Wilhein, S. Rehbein, D. Hambach, M. Berglund, L. Rymell, and H. M. Hertz, *Rev. Sci. Instrum.* **70**, 1694 (1999).

³¹L. F. Delgado-Aparicio, D. Stutman, K. Tritz, M. Finkenthal, R. Bell, D. Gates, R. Kaita, B. LeBlanc, R. Maingi, H. Yuh, F. Levinton, and W. Heidbrink, *Plasma Phys. Controlled Fusion* **49**, 1245 (2007).